



NNI FOR TREATMENT OF MULTI-DRUG RESISTANT HIV

Field of the Invention:

The invention relates to inhibitors of reverse transcriptase effective against mutant strains of HIV and effective in the treatment of multi-drug resistant HIV infection.

Background of the Invention:

Agents currently used to treat HIV infections attempt to block replication of the HIV virus by blocking the reverse transcriptase or by blocking the HIV protease. Three categories of anti-retroviral agents in clinical use are nucleoside analogs (such as AZT), protease inhibitors (such as nelfinavir), and the recently introduced non-nucleoside reverse transcriptase inhibitors (NNI) such as nevirapine.

The recent development of potent combination anti-retroviral regimens have significantly improved the prognosis for persons with HIV and AIDS. Combination therapies may be a significant factor in the dramatic decrease in deaths from AIDS (death rate as well as absolute number). The most commonly used combinations include two nucleoside analogs with or without a protease inhibitor.

Nevirapine is currently the only NNI compound which has been used in combination with AZT and/or protease inhibitors for the treatment of HIV. A new series of effective drug cocktails will most likely involve other NNIs in combination with nucleoside and protease inhibitors as a triple action treatment to combat the growing problem of drug resistance encountered in single drug treatment strategies.

The high replication rate of the virus unfortunately leads to genetic variants (mutants), especially when selective pressure is introduced in the form of drug treatment. These mutants are resistant to the anti-viral agents previously administered to the patient. Switching agents or using combination therapies may decrease or delay resistance, but because viral replication is not completely suppressed in single drug treatment or even with a two drugs combination, drug-resistant viral strains ultimately emerge. Triple drug combinations employing one (or two) nucleoside analogs and two (or one) NNI targeting RT provide a very promising therapy to overcome the drug resistance problem. RT mutant strains resistant to such a triple action drug combination would most likely not be able to function.

Dozens of mutant strains have been characterized as resistant to NNI compounds, including L1001, K103N, V106A, E138K, Y181C and Y188H. In particular, the Y181C and K103N mutants may be the most difficult to treat, because they are resistant to most of NNI compounds that have been examined.

5 Recently, a proposed strategy using a knock-out concentration of NNI demonstrated very promising results. The key idea in this strategy is to administer a high concentration of NNI in the very beginning stages of treatment to reduce the virus to undetectable levels in order to prevent the emergence of drug-resistant strains. The ideal NNI compound for optimal use in this strategy and in a triple action combination must meet three criteria:

- 10 1) very low cytotoxicity so it can be applied in high doses;
2) very high potency so it can completely shut down viral replication machinery before the virus has time to develop resistant mutant strains; and
3) robust anti-viral activity against current clinically observed drug resistant mutant strains.

15 Novel NNI designs able to reduce RT inhibition to subnanomolar concentrations with improved robustness against the most commonly observed mutants and preferably able to inhibit the most troublesome mutants are urgently needed. New antiviral drugs have the following desired characteristics: (1) potent inhibition of RT; (2) minimum cytotoxicity; and (3) improved ability to inhibit known drug resistant strains of HIV. Currently, few anti-HIV agents
20 possess all of these desired properties.

Two non-nucleoside inhibitors (NNI) of HIV RT that have been approved by the US Food and Drug Administration for licensing and sale in the United States are nevirapine (dipyrindodiazepinone derivative) and delavirdine (bis(heteroaryl)piperazine (BHAP) derivative, BHAP U-90152). Other promising new non-nucleoside inhibitors (NNIs) that have been
25 developed to inhibit HIV RT include dihydroalkoxybenzylloxypyrimidine (DABO) derivatives, 1-[(2-hydroxyethoxy)methyl]-6-(phenylthio)thymine (HEPT) derivatives, tetrahydrobenzondiazepine (TIBO), 2',5'-Bis-*O*-(tert-butyl dimethylsilyl)-3'-spiro-5''-(4''-amino-1'',2''-oxathiole-2'',2''-dioxide)pyrimidine (TSAO), oxathiin carboxanilide derivatives, quinoxaline derivatives, thiadiazole derivatives, and phenethylthiazolylthiourea (PETT)
30 derivatives.

NNIs have been found to bind to a specific allosteric site of HIV- RT near the polymerase site and interfere with reverse transcription by altering either the conformation or mobility of RT, thereby leading to a noncompetitive inhibition of the enzyme.

A number of crystal structures of RT complexed with NNIs have been reported (including
5 α -APA, TIBO, Nevirapine, and HEPT derivatives), and such structural information provides the basis for further derivatization of NNI aimed at maximizing binding affinity to RT. However, the number of available crystal structures of RT NNI complexes is limited.

Given the lack of structural information, alternate design procedures must be relied upon for preparing active inhibitors. One such method which provides important information about
10 predicting inhibitor interactions is receptor-targeted molecular modeling which heavily relies on the integrated information from crystal structures. The inclusion of such modeling information in the drug design process is likely to contribute to a more efficient identification of promising non-nucleoside inhibitors of HIV RT.

In the design of novel inhibitors, it is our working hypothesis that by examining multiple
15 crystal structures of RT-NNI complexes can one understand precisely how the NNI pocket can adjust to accommodate the binding of a particular NNI. Our composite binding pocket, unlike a single crystal structure, is able to summarize the nature and extent of the flexibility of the active site residues in the NNI binding site of RT. This allowed the *de novo* design of PETT compounds after positioning the compounds into the NNI active site of RT.

As described in copending U.S. Patent Application Serial No: 09/040,538, two major
20 features observed from the composite binding pocket model are previously unidentified spacious regions and polar regions at the Wing 2 portion of the binding pocket. It was postulated that the spacious or flexible regions of the binding pocket can accommodate and interact favorably with functional groups larger than a pyridyl ring at the Wing 2 region. Polar regions of the binding
25 pocket would interact favorably with properly positioned polar groups on the inhibitor molecule, such as halogen groups.

Using the composite binding pocket model, a series of potent NNI compounds was synthesized and assayed for anti-viral activity. These compounds abrogated HIV replication in HTLVIII-infected peripheral blood mononuclear cells at nanomolar concentrations ($IC_{50}[p24] =$
30 $<1nM$) without evidence of cytotoxicity ($IC_{50}[MTA] > 100\mu M$). Surprisingly, several compounds

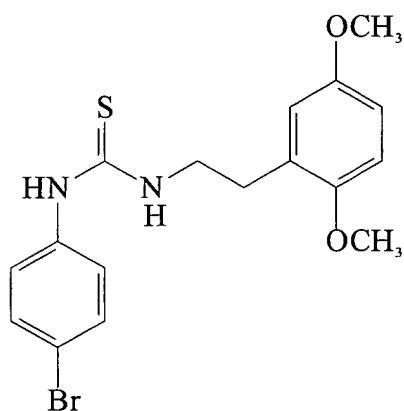
also demonstrated high potency against multiple drug resistant mutant strains, as discussed below and claimed herein.

SUMMARY OF THE INVENTION

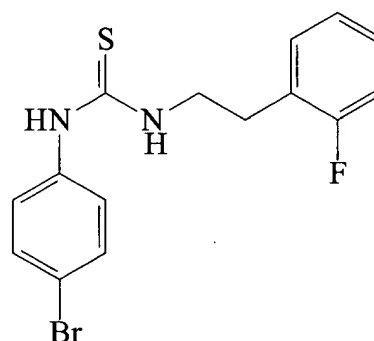
5

Non-nucleoside inhibitors of HIV reverse transcriptase have been identified, that show particular efficacy against multiple strains of HIV, including mutant strains. The compounds of the invention were designed to interact with a composite NNI binding pocket model such that the compounds better fill spacious regions in the Wing 2 region and/or favorably interact with polar residues positioned in the Wing 2 region.

Particularly potent NNI compounds of the invention include DDE236 and DDE240, having the structural formulas shown below. DDE236 contains methoxyl groups at positions 2' and 5' of the phenyl ring, filling available space in the Wing 2 region of the composite binding pocket. DDE240 contains a fluoro group at position 2' or 6' of the phenyl ring, providing a group to interact favorably with the polar region of the Wing 2. These compounds are useful in the treatment of HIV infection, and have particular efficacy against mutant strains, making them useful in the treatment of multi-drug resistant HIV.



DDE236



DDE240

The compounds of the invention, including DDE 236 and DDE240 exhibit:

- 1) very low cytotoxicity;

- 2) very high potency; and
- 3) potent activity against clinically observed drug resistant mutant strains.

5 BRIEF DESCRIPTION OF THE DRAWINGS:

Figure 1 is a photograph showing inhibitors docked into the NNI binding site of HIV-1 RT, and illustrating how the V106A mutation of RT can decrease the van der Waals contact with the inhibitor. NNIs are shown as stick models. Molecular surfaces of the compounds were prepared and color-coded based on distance calculations between the molecular surface of the NNI binding pocket and the molecular surface of the inhibitor using the GRASP program. Blue indicates the molecular surface is in van der Waals contact with RT residues; yellow indicates the surface area is not in van der Waals contact with RT; red indicates decreased van der Waals contact with RT when V106 is mutated to alanine (MDR RT). Docked molecules include: (A) DDE240; (B) DDE236; (C) DDE280; (D) DDE281; (E) nevirapine; (F) delavirdine; and (G) MKC-422.

Figure 2A is a photograph showing DDE236 in the composite binding pocket model. The Wing 2 region is on the right side of the figure.

Figures 2B-2C are X-ray crystal structures of DDE236 (B); and DDE241 (C). 30% probability displacement ellipsoids, T=20 C.

DETAILED DESCRIPTION OF THE INVENTION:

Definitions:

When used herein, the following terms have the indicated meanings:

"NNI" means non-nucleoside inhibitor. In the context of the invention, non-nucleoside inhibitors of HIV reverse transcriptase (RT) are defined.

"Composite Binding Pocket" means the model of the NNI binding site of HIV RT described in copending U.S. Patent Application 09/040,538.

"Mutant HIV" means a strain of HIV having one or more mutated or altered amino acids as compared with wild type.

"Multi-Drug Resistant HIV" means HIV infection which is resistant to treatment with one or more chemotherapeutic agent.

The Composite NNI Binding Pocket

In the search for subnanomolar NNIs-of HIV RT, it was discovered that each reported crystal structure of an RT–NNI complex has a unique binding pattern specific to one chemical class of inhibitors. Considering the limited inhibitor binding knowledge gained from one such structure, it was reasoned that rational drug design efforts should rely on as many crystal structures as possible for maximum design benefit. In this context, it is noteworthy that an analysis of the RT–APA (α -anilinophenylacetamide) structure failed to predict that the chemically dissimilar inhibitor TNK (6-benzyl-1-benzyloxymethyl uracil) could bind in the same region. The RT–APA structure predicts that there would not be enough room in the APA binding site for the 1-benzyloxymethyl group of TNK. Nevertheless, TNK is now known to bind in this region as evidenced by the crystal structure of RT–TNK which shows that RT residues can adjust to accommodate the 1-benzyloxymethyl group.

Conversely, an analysis of the RT–TNK complex does not predict favorable binding of APA in the TNK binding site. The structure does not show how residue E138 could move to accommodate the 2-acetyl group of the α -APA inhibitor. Thus, any NNI binding pocket model based on an individual RT–NNI crystal structure would have limited potential for predicting the binding of new, chemically distinct inhibitors.

To overcome this problem, a method was devised to combine the NNI binding site coordinates of nine RT–NNI crystal structures and to generate a composite molecular surface. The composite model revealed a new NNI binding pocket, as described in copending U.S. Patent Application Serial No: 09/040,538. This pocket contains the features not shown or predicted by any of the individual structures alone (Figure 1).

The composite binding pocket model information showing chemical preference for interactions between inhibitor and binding pocket was implemented to predict favorable interactions (hydrophilic, hydrophobic, hydrogen-bonding) and to facilitate the design of novel inhibitors. The surface of the binding pocket was color-coded accordingly to represent these 3 different regions: hydrophilic, hydrophobic, and hydrogen-bonding regions. As detailed in copending application U.S. Patent Application Serial No: 09/040,538, the resulting model, termed the "composite binding pocket model", provided an effective method for selecting favorable substituents on the inhibitor molecules, not only by size but also by chemical nature.

This novel composite binding pocket was used, together with a computer docking procedure and a structure-based semi-empirical score function, as a guide to predict

energetically favorable positions of new NNI compounds in the NNI binding site of RT. A number of computational tools were developed; which provided a cogent explanation for the relative activity differences among known compounds and revealed several potential ligand derivatization sites for generating new inhibitors.

5

Prediction of RT Inhibition Against Drug-resistant Mutants

The modeling studies revealed some important details regarding RT mutations leading to NNI resistance. One observation is that the Wing 2 region of the composite binding pocket consists of multiple aromatic residues including Y181, Y188 and W229. Residues Y181 and Y188 occupy a substantial volume within the binding pocket. Any mutations at Y181 or Y188 would provide a smaller residue in the Wing 2 region, which is indeed the case for Y181C, Y188C, and Y188H mutations in drug-resistant HIV strains. These mutations occupy a smaller volume of Wing 2, leading to a larger unoccupied volume in the binding pocket. An inhibitor which lacks a compatible functional group to interact with the mutated residues of Y181C, Y188C, and Y188H (a nonpolar group for Y181C and Y188C; and an aromatic group for Y188H) and which lacks a large enough group to provide surface contact with the mutated region, could result in drug resistance. This may explain the poor activity of nevirapine and delavirdine against the Y181C RT mutant (Table 2).

As for other RT mutants, the V106A mutation introduces a smaller aliphatic residue which leads to a slightly larger binding pocket volume in this region. As is the case for the Y181 and Y188 mutants, an inhibitor which does not sufficiently fill the additional volume in the V106A mutant binding pocket with a compatible (hydrophobic) functional group and which does not provide adequate van der Waal's contact with A106 may result in lower activity against the V106A RT mutant. For example, V106A can exhibit reduced van der Waals contact between the linker region located between Wing 1 and Wing 2 and the NNI compound nevirapine or delavirdine. This loss of hydrophobic contact considerably reduces, but does not abolish, the RT inhibitory activity of the NNI (Table 2). Notably, delavirdine was shown to be more potent than nevirapine against all mutants tested and against the wild type RT. Residue K103 of the wild type RT occupies a distinct volume of the binding site and possesses an electrostatic property allowing interaction with DDE192 which may be important for the stabilization of the K101 loop. The K101 loop is in close contact with nevirapine and delavirdine, and any alterations in

this region (i.e., the K103N mutation) can cause weaker binding and result in RT resistance to these drugs.

It would be advantageous to maximize the contact between NNI and the Wing 2 residues. This can be accomplished by designing inhibitors which incorporate information gained from our composite binding pocket model, including that discussed above. Resulting drugs designed with the modeling information, such as DDE236 and DDE240 have an inherent advantage in their ability to inhibit both wild-type RT as well as RT having mutations at Wing 2 (Table 2).

Designed inhibitors DDE236 and DDE240 were predicted to have significant activity against Wing 2 mutations such as Y191C and Y198C which render most NNIs inactive. In contrast, the V106A mutant is not predicted to effect the RT inhibitory activity of these compounds significantly.

Table 1.

Modeling Analysis of PETT Compound with Drug-Resistant Mutation of Residues in RT NNI binding Pocket With Side chains Directly Involved in NNI Binding.

RT NNI	Residue	Drug Mutants	Reduced Activity	Mutants
		DDE236 ^c	DDE240	
Wing 1	K103	K103N	-10 fold	Hydrogen
Wing 1	V106	V106A	0 fold	0
Wing 1	V179	V179D,E	0 fold	no change
Wing 1	P236	P236L	+4 fold	Hydrophobic
Wing 1	Y318	No ^a	—	—
Linker	L100	L100I	1.5fold	Hydrophobic
Linker	L234	No ^a	—	—
Wing 2	P95	No ^a	—	—
Wing 2	Y181	Y181C,I	—	—
Wing 2	Y188	Y188C,H,LL	10 fold	Hydrophobic
Wing 2	W229	No ^a	20 fold	Hydrophobic

Referring to Table 1, no NNI-resistant mutation has been reported. Mutants were selected via treatment by Nevirapine, Delavirdine and Efavirenz; Changes in RT inhibition against some RT mutants have been reported and are listed in Table 1. A calculated change of RT inhibition against mutants based on the composite binding pocket model using the same procedure as was applied to the Ki prediction of our designed compounds (docking procedure and modified LUDI score function). The data indicated that the K103N mutation will result in a structural loss in the charge interaction with residue DI 92; the charge pair is critical to keep the K103-containing loop in place to form a hydrogen bond with NNI. The P236L mutant is

unlikely to be selected by DDE236 and DDE240 because of the predicted enhanced inhibition due to the gain of hydrophobic contact (P236L).

It was postulated that the lead compound DDE240: N-[2-(2-fluorophenethyl)]-N'-[2-(5-bromo-pyridyl)]thiourea, (Vig et.al, 1998, *Bioorg & Med. Chem.*, 6:1789) would be effective against HIV RT mutants. DDE240 was predicted to interact more favorably with RT mutants than other compounds such as nevirapine or delavirdine. The activity of DDE240, which contains a 2'-fluoro group (Figure 1C) against wild type HIV RT was compared with compounds which contained fluoro substitutions at other positions on the phenyl ring (3'-F and 4'-F). DDE240 was shown to be the most active compound in enzyme assays measuring inhibition of recombinant RT (IC₅₀RT=0.6μM), followed by the 3'-F compound DDE241 (IC₅₀RT=0.76μM), and lastly, 4'-F, DDE242 (IC₅₀RT=6.06μM).

HIV replication assays using peripheral blood mononuclear cells infected with the NNI-sensitive HIV strain HTLV IIIB showed a similar trend, with IC₅₀[p24] values <1nM for 2'-F (DDE240) and 10nM for the 4'-F compound. DDE240 was more potent than PETT derivatives DDE253, DDE445, DDE172, and DDE276, and more potent than the S-DABO compounds DDE280 and DDE281 against both wild type RT and MDR RT (see Table 2). The inhibition trend for compounds tested against recombinant wild type RT was consistent with the inhibition trend for MDR RT.

Modeling analysis further revealed that the extensive contact of the V106 residue with the alkylthio group of S-DABO derivatives (DDE280 and DDE281) constitutes additional van der Waals contact which is lost upon mutation to MDR RT. Because the van der Waals contact loss is more pronounced for the S-DABO derivatives for the PETT compounds (DDE240, DDE241, and DDE253), the compounds DDE280 and DDE281 are predicted to have a lower activity against MDR RT. The molecular modeling is consistent with the measured IC₅₀ values, showing relatively poor performance of DDE280 and DDE281 against MDR RT (Table 2).

The lead compound, DDE240 was more active than trovirdine (Table 2). Trouviridine was three times less potent than DDE240 against the multiple drug resistant mutant strain of HIV RT (Table 2), which may reflect the fact that troviridine lacks a polar ring substituent that can provide more favorable interactions with binding site residues. The polar character of the Wing 2 residues of RT that can interact favorably with the 2'-F group of

DDE240 in the binding site would be unaffected by the clinically observed mutants K103N, V106A, Y181C DDE240 (see Figure 1D). Therefore, the favorable interaction of the binding pocket with the 2'F group of this inhibitor would not be lost in these mutants. In addition, since DDE240 was 100– to 1000–fold more potent than delaviridine or nevirapine against WT RT, a decrease in DDE240 potency against an RT mutant would likely still leave DDE240 as a relatively potent inhibitor, which may not be the case for the inherently less potent compounds such as nevirapine and delaviridine.

Modeling analysis indicated the Y181 residue stacks in a favorable herringbone orientation with the aromatic residue of NNI compounds such as DDE240. The Y181 stacking interaction is lost in the Y181C mutant, which is predictive of some degree of resistance against DDE240, delaviridine, and nevirapine. The activity of DDE240 against the Y181C mutant was 200–times better ($IC_{50}=0.2\mu M$) than delaviridine ($IC_{50}=50\mu M$), and more than 500 times more potent than nevirapine ($IC_{50}>100\mu M$).

The MDR mutant strain contains one mutation, V106A, which is located in the NNI binding pocket. Because delaviridine, nevirapine, and DDE240 all have a central portion of the molecule which is in contact with RT residue 106, they appear to show comparably lower activities against this mutant. However, the degree of resistance differed for the three compounds. DDE240 showed 100–fold better activity ($IC_{50}\mu M=0.006\mu M$) against MDR HIV than delaviridine ($0.4\mu M$) and an 800 fold better activity than nevirapine ($5\mu M$).

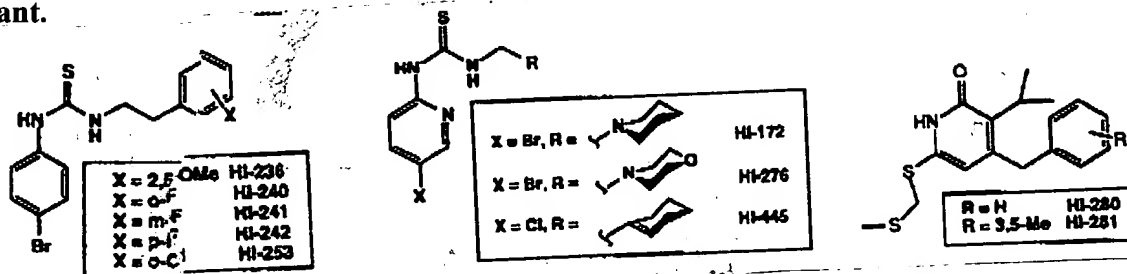
Analysis of the fit of the NNI and other inhibitors in the composite binding pocket demonstrated that the Wing 2 region has substantial molecular volume (approximately 160 cubic angstroms) surrounding the phenyl ring, defining a space that could potentially be more efficiently occupied with a larger functional group. Novel thiourea compounds were designed to optimize van der Waals contact with the binding pocket, predicting improved potency against WT RT and improved inhibition profile against Wing 2 mutants of RT. DDE236 was synthesized as a compound with one methoxy group at the 2' position (same as the fluoro atom of DDE240) and a second methoxy group at the 5' position of the phenyl ring which can contact the Wing 2 region (see Figure 1B).

Analysis of the docking of DDE236 in the NNI binding site showed that the unoccupied volume with this inhibitor was 135 cubic angstroms, a decrease of 25 cubic angstroms relative to the unoccupied volume surrounding DDE240. (See figures 1C–1D). These docking results are

consistent with the activity data showing an improved potency for DDE236, correlating to improved contact with the binding site residues.

11

Table 2: Inhibitory activity of DDE236 and DDE240 on p24 production in peripheral mononuclear cells infected with HIV strains HTLV-III_B, RT-MDR, A17, and A17 variant.



RT Inhibitors	RRT (μM)	HTLV III _B WT	RT-MDR (74V, 41L, 106A, 215Y)	A17 (Y181C)	A17 variant (Y181C, K103N)
		IC ₅₀ p24 (μM)	IC ₅₀ p24 (μM)	IC ₅₀ p24 (μM)	IC ₅₀ p24 (μM)
DDE236	0.1	<0.001	0.005	0.1	11
DDE240	0.6	<0.001	0.005	0.2	41
DDE241	0.7	<0.001	0.02	N.D.	N.D.
DDE242	6.4	N.D.	N.D.	N.D.	N.D.
DDE253	0.7	<0.001	0.004	N.D.	N.D.
DDE445	3.7	0.003	N.D.	N.D.	N.D.
DDE172	5.8	<0.001	>1	N.D.	N.D.
DDE276	>10	3.8	>1	N.D.	N.D.
DDE280	5.6	<0.001	28	>100	>100
DDE281	7.0	0.016	7	38	55
Delavirdine	1.5	0.009	0.4	50	>100
Nevirapine	23	0.034	5	>100	>100
MKC-442	0.8	0.004	0.3	N.D.	N.D.
Trovirdine	0.8	0.007	0.02	N.D.	N.D.
AZT	N.D.	0.004	0.15	0.006	0.004

N.D.= not determined; WT=wild type.

10 The synthesis of DDE172, DDE240, DDE241, DDE253, DDE280; and DDE281 and their activities against WT RT expressing the HTLV III_B strain of HIV-1 was previously reported

(Vig et.al, 1998, *Bioorg & Med. Chem.*, 6:1789; Sudbeck et.al., 1998, *Antimicro. Agents & Chemotherapy*, 42:3225; and Vig et.al., 1998, *Bioorg. & Med. Chem. Lett.* 8:1461).

5 Design and Modeling Analysis of DDE236

A computer simulation of the binding of DDE236 into the NNI binding site of RT was accomplished using a molecular docking procedure. Docking of these compound into the NNI binding site required the use of X-ray coordinates of an RT/NNI complex (in this case the RT/9CL-TIBO complex). Upon binding to RT, the compound can fit into a butterfly-shaped NNI binding site (described by Ding et.al., 1995, *Nat. Struct. Biolog.* 11:1122 (Figures 1A and 2A)). Once the final docked position of the molecule in the NNI site was determined, the molecule was assigned a score, from which an estimation of the inhibition constant (K_i value) was determined. When trovirdine was docked into the NNI binding site of RT it had a higher binding score than PETT and fit into the butterflyshaped binding region with one part residing in Wing I and the other in Wing 2. The ring closest to the thiocarbonyl group resided near the Lys(K) 101 loop and the other pyridyl ring was near Trp(W)229.

After docking and K_i estimation was completed for the trovirdine, evaluation of the docked compounds in the active site of RT involved placing each compound into the composite binding pocket using the same orientation matrix utilized in its construction. The potentially flexible regions in the binding site were then readily identified as were atom sites for future derivatization of the compounds. The area within Wing 2 and the residues near the thiourea group seemed to be the most forgiving regions in the binding site of RT. It was postulated that a more efficient use of such sterically allowed unoccupied spatial gaps in the binding site could be achieved by replacing the 2-pyridyl ring of trovirdine with a 2,5-dimethoxyphenyl moiety (DDE236) and yield potentially more active PETT compounds with larger molecular surface areas, higher Ludi scores, and lower K_i values.

The molecular surface area of the compounds after docking was calculated. At docked positions, the atom surface area in contact with the protein residues constituted an average of 84% of the entire molecular surface. We used this average value in the calculation of the inhibitory constant (k_i) based on the Ludi score function. The calculated K_i value of DDE236 (0.2 μ M) was better than those of known compounds PETT (2.4 μ M) and trovirdine (0.7 μ M).

The docking studies indicated that the 2-methoxy group of DDE236 is situated beneath the ethyl linker and fits favorably into a cavity of the binding pocket, providing contact with protein residues that cannot be achieved by trovirdine. Likewise, the 5-methoxy group of DDE236 provides close contact with residues Pro95 and Trp229. The trend of the calculated K_i values appeared to predict the trend of the experimentally determined IC_{50} values from HIV replication assays (Table 2). The compound DDE236 with the lowest calculated K_i values of the series was 8-times more potent than trovirdine against purified recombinant HIV-RT using the cell-free Quan-T-RT system ($IC_{50}[rRT]$ was $0.1\mu M$ for DDE236 versus $0.8\mu M$ for trovirdine). DDE236 also elicited potent anti-HIV activity with IC_{50} values of less than $0.001\mu M$ in 3 of 3 independent experiments which was consistently lower than the IC_{50} values for trovirdine ($0.007\mu M$) and AZT ($0.004\mu M$). Furthermore, the IC_{90} value of our DDE236 (9 nM) was 10-fold better than that of AZT (100 nM). None of the PETT derivatives were cytotoxic at concentrations as high as $100\mu M$. Therefore, the calculated selectivity index ($IC_{50}[MTA] / IC_{50}[p241]$) of DDE236 was $> 10^5$.

The same modeling procedure was applied to RT mutants (Table 1). DDE236 was predicted to have better K_i value than the trovirdine against the RT mutants examined (Table 2) for the following reasons. DDE236, which contain larger functional group which can contact the Wing 2 region of RT (based on our composite binding pocket model) will not only have significant potency against wild-type RT but will also show high potency against many RT mutants such as Y181 C which is resistant to many examined NNI inhibitors currently in clinical use.

Design and, Modeling Analysis of DDE240

Similar to the design of DDE236, the design of DDE240 was also focused on improving its interaction with the Wing 2 region. However, instead of using large group to better contact with binding pocket, the fluoro atom was used to improve the contact with the binding pocket based on compatible chemical nature. The position of the docked trovirdine molecule revealed multiple potential derivatization sites for incorporation of polar groups, at specific locations. The favorable regions for polar groups were readily identified by blue color-coding on the surface of the binding pocket model. The 3'-position on the

pyridyl ring of trovirdine (equivalent to the *ortho* or C2 position of a phenyl derivative) would be a good location for a fluorine atom because it could interact favorably with nearby polar residues in the composite binding pocket (Figure 1). The 5' position on the pyridyl ring (*para* or C4 position of a phenyl derivative) of trovirdine would be near a hydrophobic region however, making it a poor location for a fluorine substituent. DDE240 with fluoro substituent at *ortho* position on the ring was synthesized and tested for anti-HIV activities.

Coordinates of DDE240 were generated and positioned into the crystal structure coordinates of the RT/9-Cl-TIBO active site by a docking procedure (Methods) identical to that used for DDE236. The main conformational difference between the energy-minimized model of DDE240 and its crystal structure is a 120° rotation around the ethyl linker, which could be stabilized by favorable contacts with binding site residues if the molecule adopted this conformation upon binding. This conformation of the energy-minimized model of DDE240, aided by an intramolecular hydrogen, allows the molecule to fit favorably into the NNI bond (also observed in the crystal structure of binding site of RT).

After the molecules were docked into the binding site, an assessment of how well they would be predicted to bind was done. The color-coded composite binding pocket illustrating preferred regions of interaction shows that Wing 2 is mostly hydrophobic except for the region near the *ortho* positions of the phenyl ring of the inhibitor, where a polar group such as fluorine would be compatible. Substitutions at the *meta* position would be on the edge between the polar region and the hydrophobic region of the binding site. Modeling of DDE240 showed that the *ortho*-F group does interact favorably with the polar region of the binding site, which would contribute to a stronger binding to RT. The *ortho*-F group was predicted to be located near the interface between polar and hydrophobic regions of the binding site, where the *meta*-F substituent is half exposed to the polar (blue) region. This suggests that the *meta*-F group could interact favorably with the polar region only if the fluorine is in the correct orientation. If the orientation of the *meta*-F group was such that it would extend toward the hydrophobic region instead, weaker binding would result. The *para*-F group was apparently not compatible with the composite binding pocket.

The *ortho*-F substituted compound DDE240 was shown to be the most active in enzyme assays measuring inhibition of recombinant RT ($IC_{50}RT = 0.4\mu M$), followed by *meta*-F ($IC_{50}RT = 0.7\mu M$), and lastly *para*-F ($IC_{50}RT = 6.0\mu M$). The HIV replication assays using

peripheral blood mononuclear cells infected with the zidovudine-sensitive HIV strain HTLVHM showed a similar trend, with IC₅₀[p24] values < 1 nM for *o*-F DDE240 and 10 nM for the *p*-F compound. The *para*-F atom, which is small in size but electronegative, is probably compatible with the location of the ring plane of nearby hydrophobic Trp229 but offers an interaction less favorable than that of *o*-F or *m*-F. Trovirdine was shown to be 10 times less potent than DDE240 against the zidovudine-sensitive HIV strain HTLVHM and up to 7 times less potent than DDE240 against the multiple-drug-resistant mutant strain of HIV RT (Table 2), which may reflect the fact that trovirdine lacks a polar ring substituent which can provide more favorable interactions with binding site residues.

EXAMPLES

METHODS

Construction of the NNI Binding Pocket

Modeling studies required the construction of a binding pocket which encompassed all RT-NNI complexes with known crystal structures. First, a total of eight coordinates of RT complexes with the compounds HEPT, MKC, TNK, APA, Nevirapine, N-ethyl Nevirapine derivative, 9-Cl TIBO (Stuart *et al.*),²² and 9-Cl TIBO with PDB access codes rti, rtl, rt2, hni, vrt, rth, rev and tvr, respectively, were superimposed onto the full coordinates of RT complexed with 8-CITIBO (PDB access code hnv). The "thumb" region of RT complexes are relatively variable compared with the palm region. Therefore, a total of 117 C α atoms of the residues from 97 to 213 which cover part of the NNI binding site and the palm region were used for a least-squares superimposing procedure within the program. The RMS values are shown to be 1.00, 0.98, 0.99, 0.62, 0.80, 0.87, 0.94 and 0.65 Å for HEPT, MKC, TNK, APA, Nevirapine, N-ethyl nevirapine derivative and two 9-Cl TIBO complexes, respectively. The coordinates of the corresponding inhibitor molecules were then transformed according to the same matrices derived from the superimposition. Lastly, an overall molecular surface providing a binding pocket encompassing all inhibitors was generated from the overlaid non-hydrogen atom coordinates of all inhibitors using the program GRASP. The surface of the binding pocket was color-coded to reflect characteristics of the overlaid inhibitors, such as hydrogen bonding, hydrophilic, and hydrophobic regions. The nitrogens on the uracil ring of HEPT and TIBO derivatives were color coded red for hydrogen-bonding atoms. Oxygen or sulfur atoms of carbonyl, thiocarbonyl, and

ester groups, nitrogen atoms of amine groups, and halogen atoms were color-coded blue for polar (hydrophilic) groups. Carbon atoms were considered to be hydrophobic and were colored gray. This pocket, referred to as the composite binding pocket, was used as a basis for the analysis of inhibitor binding to the NNI binding site of HIV RT.

5

Docking and K_i Prediction

Fixed docking in the Affinity program within as used for docking small molecules to the NNI binding site which was taken from a crystal structure (PDB code rev, RT/9-CI-TIBO complex). The program has the ability to define a radius of residues within a 5 Å distance from the NNI molecule. As the modeling calculations progressed, the residues within the defined radius were allowed to move in accordance with energy minimization. Ten final docked positions were initially chosen for each inhibitor modeling calculation but failed to reveal more than two promising positions. Later, only two calculated positions were set for the search target. Calculations were carried out on a SGI INIDIG02 using the CVFF force field in the Discover program and a Monte Carlo search strategy in Affinity. No salvation procedures were used. Since the total number of movable atoms exceeded 200, conjugated gradient minimization was used instead of the Newton minimization method. The initial coordinates of the compounds were generated using the Sketcher module within InsightII. Each final docking position was then evaluated by a score function in Ludi. The top scoring model was then compared with the composite binding pocket and the known crystal structure of similar compounds and used for further analyses.

Several modifications were imposed during the calculation of inhibitory constants (k_i) of the positioned compounds using the Ludi score function. First, the molecular surface areas (MS) were directly calculated from the coordinates of the compounds in docked conformations using the MS program. Second, we re-evaluated the number of rotatable bonds (NR) which was assessed inaccurately by INSIGHTII (rigidity imposed by hydrogen bonding was not accounted for in the program). Third, we assumed that the conserved hydrogen bond with RT did not deviate significantly from the ideal geometry. This assumption was supported by the fact that in the known crystal structures of RT complexes, all hydrogen bonds between NNIs and RT are near the ideal geometry. Lastly, for the trovirdine compounds, we found it necessary to impose an additional penalty for a charged group or halogen atoms when positioned near the ring plane of a protein residue such as tryptophan 229 because the interaction was not adequately accounted

for in the Ludi score. The working modification of the Ludi scoring function for the PETT compounds included subtracting a score of P from the total Ludi score when the ring plane of the Trp229 was within 5 Å distance from a *para* substituent (R):

$$\text{Ludi Score} = \text{MS} * \text{BS} * 2.93 + 95 (\text{H-bond}) - \text{NR} * 24.2 - 100 - \text{P};$$

5 Where P=200, when R=a hydrophilic group, e.g. -OH or -NO₂;

P=100, when R=a *para*-halo atom, e.g. -F, -Cl or -Br;

P=50, when R= a *para*-methoxy, e.g. -OMe;

P=0, when R= a hydrophobic group, e.g. H, CH₃;

Consequently, the K_i values for the modeled compounds were more predictable than they
10 would be otherwise without such modification.

Chemistry

All chemicals were purchased from the Aldrich Chemical Company (Milwaukee, WI). Anhydrous acetonitrile and N,N-dimethylformamide were obtained from Aldrich in sure seal bottles and were transferred to reaction vessels via cannula under nitrogen. All reactions were carried out under the atmosphere of nitrogen. Nuclear magnetic resonance (NMR) spectra were recorded on a Varian 300 MHz instrument and chemical shifts are reported in parts per million (ppm) relative to tetramethyl silane as an internal standard. Splitting patterns are designated as follows: s = singlet, d = doublet, t = triplet, q= quartet, m = multiplet, br = broad peak. ¹³C NMR spectra were recorded in CDCl₃ on the same instrument using the proton decoupling technique. The chemical shifts reported for ¹³C NMR are referenced to chloroform at 77.0 ppm. NMR spectra were recorded in CDCl₃ and a 1% solution of trifluoroacetic acid in water was used as an internal standard in a fused capillary tube. Melting points were obtained using a Fisher-Johns melting
25 apparatus and are uncorrected. UV spectra were recorded from a Beckmann Model # DU 7400 UVNis spectrometer using a cell path length of 1 cm. Fourier transform infrared spectra were recorded using an FF-Nicolet model Protege #460 instrument. Mass spectra analysis were conducted using a Hewlett-Packard Matrix Assisted Laser Desorption Time-of-Flight (MALDI-TOF) spectrometer model # G2025A. The matrix used was cyanohydroxycinnamic
30 acid. Column chromatography was performed using EM Science silica gel 60. The solvents used for elution varied depending on the compound and included one of the following: ethyl

acetate, methanol, chloroform, hexane, methylene chloride or ether. Elemental analysis was performed by Atlantic Microlabs (Norcross, GA).

N-[2-(2,5-dimethoxyphenylethyl)]-N'-[2-(5-bromopyridyl)]-thiourea (DDE236) white solid (2g, 67%); mp 133–138° C; UV (MeOH) λ_{max} : 202, 205, 231, 276 and 300 nm; IR(KBr Disc) ν 3209, 3152, 3078, 3028, 2951, 2831, 1595, 1533, 1468, 1306, 1227, 1095, 1059, 1022, 862, 825, 796, 707 cm^{-1} ; ^3H NMR(CDCl_3) δ 11.24 (br s, 1H), 9.30 (br s, 1H), 8.10–8.09 (d, 1H), 7.65 (dd, 1H), 6.82–6.76 (m, 4H), 4.03–3.97 (q, 2H), 3.77 (s, 3H), 3.76 (s, 3H), 3.00–2.96 (t, 2H); ^{14}C NMR(CDCl_3) δ 178.7, 153.1, 151.8, 151.7, 146.5, 140.9, 128.1, 117.7, 113.3, 112.6, 111.2, 110.9, 55.7, 55.5, 45.6, and 29.9; MALDI-TOF mass found, 394.0 (M–1), 396.0 (M+1), calculated, 395.0; Anal. ($\text{C}_{16}\text{H}_{18}\text{BrN}_3\text{O}_2\text{S}$) C, H, N, S, Br.

N-[2-(2-fluorophenethyl)]-N'-[2-(5-bromopyridyl)]-thiourea (DDE240) yield: 71%; mp 156–157 °C; UV (MeOH) λ_{max} : 209, 256, 274 and 305 nm; IR(KBr) ν 3446, 3234, 3163, 3055, 2935, 1672, 1595, 1560, 1531, 1466, 1390, 1362, 1311, 1265, 1227, 1169, 1136, 1089, 1003, 864, 825, 756 cm^{-1} ; ^1H NMR (CDCl_3) δ 11.36 (br s, 1H), 9.47 (br s, 1H), 8.05–8.04 (d, 1H), 7.72–7.68 (dd, 1H), 7.30–7.03 (m, 4H), 6.87–6.84 (d, 1H), 4.06–3.99 (q, 2H), 3.10–3.05 (t, 2H); ^{14}C NMR(CDCl_3) δ 179.1, 163.1, 151.7, 146.2, 141.1, 131.2, 131.1, 128.5, 128.4, 124.1, 115.5, 115.2, 113.6, 112.2, 45.8 and 28.2; ^{19}F NMR(CDCl_3) δ –42.58 & 42.55 (d); Maldi ToF found: 355.0 (M+I), calculated: 354.0; Anal. ($\text{C}_{14}\text{H}_{13}\text{BrFN}_3\text{S}$) C, H, N, S.

General procedure for synthesis

Compounds were synthesized according to **Scheme 1**. In brief, 2-amino-5-bromopyridine was condensed with 1, I –thiocarbonyl diiniidazole to furnish the precursor thiocarbonyl derivative (A). Further reaction with appropriately substituted phenylethyl amine gave the target PETT derivatives in good yields.

Specifically, thiocarbonyldiiniidazole (8.90g, 50 mmol) and 2-amino-5-bromo pyridine (8.92g, 50 mmol) were added to 50 mL of dry acetonitrile at room temperature. The reaction mixture was stirred for 12 h and the precipitate filtered, washed with cold acetonitrile (2x25 mL), and dried under vacuum to afford (I 1.40g, 80 %) of compound A. To a suspension of compound A (0.55eqv) in dimethyl formamide (15mL)

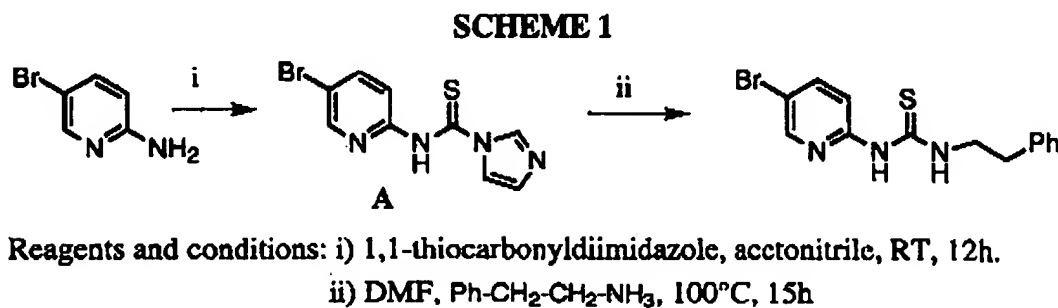
an appropriate amine (0.50eqv) was added. The reaction mixture was heated to 100°C and stirred for 15 h. The reaction mixture was poured into ice-cold water and the suspension was stirred for 30 min. The product was filtered, washed with water, dried, and further purified by column chromatography to furnish the target compounds 1–9 in good yields.

5

Purified RT Assays for Anti-HIV Activity

Compounds **3a–3d** were tested for RT inhibitory activity (IC₅₀[rRT]) against purified recombinant HIV RT using the cell-free Quan-T-RT system (Amersham, Arlington Heights, IL), which utilizes the scintillation proximity assay principle.³⁸ In the assay, a DNA/RNA template is bound to SPA beads via a biotin/streptavidin linkage. The primer DNA is a 16-mer oligo(T) which has been annealed to a poly(A) template. The primer/template is bound to a streptavidin-coated SPA bead.

3H-TTP is incorporated into the primer by reverse transcription. In brief, 3H-TTP, at a final concentration of 0.5 µCi/sample was diluted in RT assay buffer (49.5 mM Tris-Cl, pH 8.0, 80 mM KCl, 10 mM MgCl₂, 10 mM DTT, 2.5 mM EGTA, 0.05% Nonidet-P-40), and added to annealed DNA/RNA bound to SPA beads. The compound being tested was added to the reaction mixture at 0.001 µM–100 µM concentrations. Addition of 10 mU of recombinant HIV RT and incubation at 37°C for 1 hour resulted in the extension of the primer by incorporation of 3 H-TTP. The reaction was stopped by addition of 0.2 ml of 120 mM EDTA. The samples were counted in an open window using a Beckman LS 7600 instrument and IC₅₀ values were calculated by comparing the measurements to untreated samples.



p24 Assays for Anti-HIV Activity

Normal human peripheral blood mononuclear cells (PBMNC) from HIV-negative donors were cultured 72 hours in RPMI 1640 supplemented with 20%(v/v) heat-inactivated fetal bovine serum (FBS), 3 % interleukin-2, 2 mM L-glutairtine, 25 mM HEPES, 2 μ L, NAHCO,
5 50 mg/mL gentamicin, and 4 μ g/mL phytohemagglutinin prior to exposure to HIV- I at a multiplicity of infection (MOI) of 0. 1 during a one-hour adsorption period at 37°C in a humidified 5% CO₂ atmosphere. Subsequently, cells were cultured in 96-well microliter plates (100 μ l/well; 2x 10⁶ cells/mL, triplicate wells) in the presence of various inhibitor concentrations and aliquots of culture supernatants were removed from the wells on the 7th day
10 after infection for p24 antigen p24 enzyme immunoassays (EIA), as previously described. (see Erice et.al., 1993, *Antiimicrob. Ag. Chemotherapy* 37:835-838) The applied p24 EIA was the unmodified kinetic assay commercially available from Coulter Corporation/Immunotech, Inc. (Westbrooke, ME), which utilizes a murine monoclonal antibody to HIV core protein coated onto microwell strips to which the antigen present in the test culture supernatant samples binds. Percent inhibition of viral replication was calculated by comparing the p24 values from the test substance treated infected cells with p24 values from untreated infected cells (i.e., virus controls). In parallel, the effects of various treatments on cell viability were also examined, as described in Enrice et.al., supra. In brief, non-infected PBNWC were treated with each compound for 7 days under identical experimental conditions. A Microculture Tetrazolium Assay (NTFA), using 2,3-
20 bis(2-methoxy-4 nitro-5-sulfophenyl)-5-[(phenylarnino)-carbonyl]-2H-tetrazolium hydroxide (XTT), was performed to quantitate cellular proliferation.

CONCLUSIONS

25 Novel molecules DDE236 and DDE240, namely N-[2-(2,5-dimethoxyphenylethyl)] - N'- 2-(5-bromopyridyl)]-thiourea and N-[2-(2-fluorophenylethyl)]-N'-[2(5-bromopyridyl)]-thiourea have been designed. These compounds exhibit unprecedented picomolar potency against HIV RT wild-type and drug-resistant mutants (Table 2). The design strategy was based on taking full advantage of the previously identified space in the composite binding pocket
30 model and modeling of clinically identified mutation in the NNI binding pocket. These NNI

compounds exhibit anti-HIV activity superior to that of the parent compounds and are more effective against drug-resistant strains of HIV.

5 This specification makes reference to numerous patent and literature citations, each of which is hereby incorporated by reference for all purposes as if fully set forth in the text.

112
113
114
115
116
117
118
119
120
121
122
123
124
125
126
127
128
129
130
131
132
133
134
135
136
137
138
139
140
141
142
143
144
145
146
147
148
149
150
151
152
153
154
155
156
157
158
159
160
161
162
163
164
165
166
167
168
169
170
171
172
173
174
175
176
177
178
179
180
181
182
183
184
185
186
187
188
189
190
191
192
193
194
195
196
197
198
199
200
201
202
203
204
205
206
207
208
209
210
211
212
213
214
215
216
217
218
219
220
221
222
223
224
225
226
227
228
229
230
231
232
233
234
235
236
237
238
239
240
241
242
243
244
245
246
247
248
249
250
251
252
253
254
255
256
257
258
259
260
261
262
263
264
265
266
267
268
269
270
271
272
273
274
275
276
277
278
279
280
281
282
283
284
285
286
287
288
289
290
291
292
293
294
295
296
297
298
299
300
301
302
303
304
305
306
307
308
309
310
311
312
313
314
315
316
317
318
319
320
321
322
323
324
325
326
327
328
329
330
331
332
333
334
335
336
337
338
339
340
341
342
343
344
345
346
347
348
349
350
351
352
353
354
355
356
357
358
359
360
361
362
363
364
365
366
367
368
369
370
371
372
373
374
375
376
377
378
379
380
381
382
383
384
385
386
387
388
389
390
391
392
393
394
395
396
397
398
399
400
401
402
403
404
405
406
407
408
409
410
411
412
413
414
415
416
417
418
419
420
421
422
423
424
425
426
427
428
429
430
431
432
433
434
435
436
437
438
439
440
441
442
443
444
445
446
447
448
449
450
451
452
453
454
455
456
457
458
459
460
461
462
463
464
465
466
467
468
469
470
471
472
473
474
475
476
477
478
479
480
481
482
483
484
485
486
487
488
489
490
491
492
493
494
495
496
497
498
499
500
501
502
503
504
505
506
507
508
509
510
511
512
513
514
515
516
517
518
519
520
521
522
523
524
525
526
527
528
529
530
531
532
533
534
535
536
537
538
539
540
541
542
543
544
545
546
547
548
549
550
551
552
553
554
555
556
557
558
559
560
561
562
563
564
565
566
567
568
569
570
571
572
573
574
575
576
577
578
579
580
581
582
583
584
585
586
587
588
589
590
591
592
593
594
595
596
597
598
599
600
601
602
603
604
605
606
607
608
609
610
611
612
613
614
615
616
617
618
619
620
621
622
623
624
625
626
627
628
629
630
631
632
633
634
635
636
637
638
639
640
641
642
643
644
645
646
647
648
649
650
651
652
653
654
655
656
657
658
659
660
661
662
663
664
665
666
667
668
669
670
671
672
673
674
675
676
677
678
679
680
681
682
683
684
685
686
687
688
689
690
691
692
693
694
695
696
697
698
699
700
701
702
703
704
705
706
707
708
709
710
711
712
713
714
715
716
717
718
719
720
721
722
723
724
725
726
727
728
729
730
731
732
733
734
735
736
737
738
739
740
741
742
743
744
745
746
747
748
749
750
751
752
753
754
755
756
757
758
759
760
761
762
763
764
765
766
767
768
769
770
771
772
773
774
775
776
777
778
779
780
781
782
783
784
785
786
787
788
789
790
791
792
793
794
795
796
797
798
799
800
801
802
803
804
805
806
807
808
809
810
811
812
813
814
815
816
817
818
819
820
821
822
823
824
825
826
827
828
829
830
831
832
833
834
835
836
837
838
839
840
841
842
843
844
845
846
847
848
849
850
851
852
853
854
855
856
857
858
859
860
861
862
863
864
865
866
867
868
869
870
871
872
873
874
875
876
877
878
879
880
881
882
883
884
885
886
887
888
889
890
891
892
893
894
895
896
897
898
899
900
901
902
903
904
905
906
907
908
909
910
911
912
913
914
915
916
917
918
919
920
921
922
923
924
925
926
927
928
929
930
931
932
933
934
935
936
937
938
939
940
941
942
943
944
945
946
947
948
949
950
951
952
953
954
955
956
957
958
959
960
961
962
963
964
965
966
967
968
969
970
971
972
973
974
975
976
977
978
979
980
981
982
983
984
985
986
987
988
989
990
991
992
993
994
995
996
997
998
999
1000